Journal of Solid State Chemistry 181 (2008) 1961–1969

Contents lists available at ScienceDirect

Journal of Solid State Chemistry

journal homepage: www.elsevier.com/locate/jssc

The higher excited electronic states and spin–orbit splitting of the valence band in three-dimensional assemblies of close-packed ZnSe and CdSe quantum dots in thin film form

Biljana Pejova *

Faculty of Natural Sciences and Mathematics, Institute of Chemistry, Saints Cyril and Methodius University, PO Box 162, 1001 Skopje, Macedonia

ARTICLE INFO

Article history:
Received 11 December 2007
Received in revised form
27 March 2008
Accepted 30 March 2008
Available online 11 April 2008

Keywords:
Zinc selenide
Cadmium selenide
Thin films
Quantum dots
Quantum dot solids
Quantum size effects
Band gap energy
Spin–orbit splitting
Optical properties
Higher excited electronic states
Semiconductors

ABSTRACT

Optical properties of as-deposited and annealed thin films composed of three-dimensional arrays of sphalerite-type ZnSe and CdSe quantum dots (QDs), synthesized by chemical deposition, were investigated. Neglecting the *S–D* mixing of hole states, the lowest "band to band" transitions in very small nanoclusters and in bulk-like clusters may be assigned as $1S \rightarrow 1S$ and $1S_{\Delta} \rightarrow 1S$, and are split by spin–orbit (SO) splitting energy of the bulk material—Δ. The splitting energy between these transitions was found to be insensitive to QD size variations, which could be explained assuming that 1*S* hole states arising from valence band Γ_7 and Γ_8 components do not mix with higher angular momentum states and shift together to higher energies coupled via the *isotropic* hole mass. This implies significant difference between the SO splitting energies in the two semiconductors. Accounting for *S–D* mixing of hole states, the observed transitions may be attributed to the fundamental ground state—$(1S_{3/2}, 1S_e)$ and the ground state—$(1S_{1/2}, 1S_e)$ ones. The observed "splittings" thus do not correspond exactly to SO splitting energy in both semiconductors, but are complex functions of it, as exact position of each hole energy level depends, besides on Δ, also on other material-characteristic parameters.

1. Introduction

Studies of nanometer-scale semiconductor crystals (quantum dots—QDs) have enabled a profound understanding of the size-evolution of semiconducting materials' electronic properties. Essentially, QDs have opened the opportunity to materials scientists to study the evolution of electronic behavior in size regime which is intermediate between "molecular" and "bulk" forms of matter [1–3]. This has led to the possibility to control and tune materials' properties. In essence of the size evolution of electronic properties are the effects of size-quantization. Quantum size effects in semiconductor QDs occur when their size is small in comparison to Bohr excitonic radius which acts as a natural length scale of the electron–hole pair. These effects are a direct consequence of the confined electron and hole motions in three spatial dimensional. A QD nanostructure is actually a zero-dimensional analog of the two-dimensional quantum well (QW) which is characterized by discretized energy level structure and discrete electronic transitions which shift to higher energies upon decrease of the QD linear dimensions. Significant effort has been devoted in the literature to understand thoroughly the influence of quantum confinement effects on QD spectroscopic properties [1,4–13]. Early approaches which treat the previous question have usually suffered from a number of oversimplifications such as taking into account only a single valence band in the model [1,5–7]. Valence bands of even structurally simple semiconductors, such as sphalerite polymorphs of ZnSe and CdSe, often show remarkable complexities [14–16]. In the case of mentioned semiconductor compounds, these complexities in hole dispersion relations are mainly due to the fact that the valence band originates from anionic *p*-orbitals. This band is therefore six-fold degenerate (counting the spin) and the effects of coupling of the spin and orbital angular momentum are very significant. Obviously, having in mind the previously outlined arguments, the purely quantum property of charge-carriers—spin, enters the semiconductor physics as a substantially important "new" variable. Actually, the spin physics of semiconductors is a rapidly expanding field of contemporary science [17–21]. A particularly explosive development has been noted in relation to spin-related optical and transport properties in low-dimensional semiconductor

* Fax: +389 2 3226 865.
E-mail address: biljana@iunona.pmf.ukim.edu.mk

0022-4596/$ - see front matter © 2008 Elsevier Inc. All rights reserved.
doi:10.1016/j.jssc.2008.03.038

structures. The spin–orbit (SO) interaction has attracted considerable attention due to a number of reasons. First of all, it enables optical spin orientation and detection. It could exhibit significant influence on the mesoscopic transport phenomena and quantum Hall effect and in most cases the SO coupling is responsible for spin relaxation phenomena. In addition to this, it introduces an interdependency between the transport and spin phenomena. The whole newly developed field of spintronics, has already offered unique opportunities for construction of a new generation of multifunctional devices which would be based on addition of the spin degree of freedom to the conventional (charge-based) microelectronics. Besides the wide field of potential applicability of phenomena related to SO coupling, research in this field is also of certain fundamental significance. While the basic physics, which governs the size-quantization effects on optical properties of low-dimensional semiconductor nanostructures, seems to be well understood in a qualitative sense (in spite of the quantitative disagreements between theory and experiments in some cases), the mechanisms governing the SO coupling as well as its strength in mentioned systems is still a very active area of research.

When individual QDs are close-packed (forming, e.g. three-dimensional assembly of QDs—a QD solid), further new opportunities are opened and fundamentally new aspects might be explored in arrays of QDs. In the case of QD solids the collective physical phenomena that develop upon interaction of the proximal QDs may be explored, while certain properties which are characteristic of individual QDs are retained [22–29]. Such unique properties characteristic of an individual QD on the one hand and the cooperative effects in QD solids on the other hand, make these novel types of superstructures as very convenient media with great potential for application in optical and electronic devices.

The higher excited electronic states in ZnSe and CdSe (as well as in ZnS) nanoclusters, with an emphasis on the SO coupling were studied by Chestnoy et al. [30]. However, these authors have focused their attention on colloidal systems of the title semiconducting materials, synthesized by arrested precipitation colloidal technique. Velumani et al. [31] have studied the optical properties of hot wall deposited CdSe thin films obtained under various experimental conditions, and in this context they also presented the energies of the higher-order electronic transitions due to SO splitting of the valence band in this semiconductor. The main emphasis in this paper was, however, put on the influence of deposition conditions on the optical transitions, because the average crystal diameters were all close to 30 nm and size-quantization effects were not exhibited by the studied films. Němec et al. [32] have utilized light-controlled chemical deposition technique for synthesis of nanocrystalline CdSe thin films. On the basis of optical absorption and photoluminescence data these authors have calculated the SO splitting energy in series of thin films with varying average crystal size deposited under different experimental conditions. Series of profound works by Norris and Bawendi [33–36], as well as Alivisatos and Brus [37], Efros [38], Xia [39] and Hodes [40,41] have been devoted to correct assignments of the higher-energy transitions detected in the photoluminescence and optical spectra of CdSe QDs in various size regimes (from strong to weak confinement). The groups of Artemyev and Woggon [24–27,42–45] have devoted particular attention to the phenomena which arise in ensembles of close-packed QD solids, specifically addressing the semiconducting CdSe QDs. The question of excitons in CdSe QDs has been theoretically addressed by Laheld and Einevoll [46]. The relation of interdot interactions to optical properties of CdSe nanocrystal arrays has been investigated in series of profound works [47–49]. A particularly interesting study related to excitonic levels of CdSe QDs embedded in an amorphous GeS_2 thin film matrix has been published by Raptis et al. [50]. These authors have observed resonant Raman effects which have been related to resonant light absorption in several excitonic transitions of the CdSe QDs.

In the present paper, we perform a systematic study of the optical absorption of close-packed variable-sized ZnSe and CdSe QDs in thin film form. We put a special emphasis on the consequences of the SO splitting of the valence band in the title compounds and the characteristics of the higher excited electronic states which arise from this effect. This work is a continuation of our previous studies related to low-dimensional semiconductors mostly deposited as thin films composed of three-dimensional assemblies of QDs [51–63]. Our interest for the title semiconducting compounds arose due to their attractiveness as promising opto-electronic materials [64–74].

2. Synthesis and identification of ZnSe and CdSe QD thin films

Thin films of close-packed semiconducting ZnSe and CdSe QDs were deposited on glass substrates by the methods developed by our group [55,58]. Both synthetic approaches are actually based on controllable chemical colloidal precipitation technique from a single solution. Sodium selenosulfate was used as precursor of selenide anions in the reaction systems, while controllably low concentrations of Zn^{2+} and Cd^{2+} ionic species were maintained using suitable complexing agents. In the case of ZnSe thin film deposition the pH of the reaction system was kept at a very high value ($\approx$14) and the OH^- ions, present in rather high concentration, served as complexing agent for Zn^{2+} ions. As explained in much more details in our paper [55], under these conditions, only a single equilibrium involving Zn^{2+} ions exists in the reaction system: the one between $[Zn(OH)_4]^{2-}$ and Zn^{2+} species, which enabled us to avoid the presence of $Zn(OH)_2$ in the reactor and its further incorporation in the ZnSe films. In the case of CdSe, ammonia buffer solution was used to maintain a constant pH value during thin film deposition process [58]. At the same time, ammonia served as a complexing agent for the Cd^{2+} ions. Since sodium selenosulfate is not commercially available, we have synthesized the precursor of selenide anions prior to the deposition processes, by the route explained in our previous works [55,58]. It is known that the hexagonal (wurtzite) phases of these two semiconducting compounds are thermodynamically the most stable ones. It is therefore a rather difficult task to synthesize their cubic (sphalerite, i.e. zinc-blende) modifications with sufficient crystallographic (phase) purity. However, as discussed in our previous works [55,58], contrary to most of the other approaches proposed in the literature, our methods enable synthesis of cubic ZnSe and CdSe polymorphs as thin films and bulk precipitates.

The deposited thin films and bulk precipitates were identified by the Debye–Scherrer method of X-ray diffraction (XRD) from polycrystalline samples. Average crystal diameters were calculated by Scherrer's algorithm [75,76]. First, Scherrer's (or coherence) length was calculated from the positions and broadenings of the XRD peaks. For precise determination of the full width at half maximum intensity of a given peak, each relevant peak was interpolated by linear combination of Gaussian and Lorentzian functions. Further, the coherence length was converted to the average crystal diameter within the spherical approximation for the shape of semiconductor nanocrystals [76]. The contribution of instrumental factors to the overall peak broadening was also taken into account by the more general form of Scherrer's formula. It was found that the as-deposited films (as well as the bulk precipitates) are highly nanocrystalline. Upon thermal treatment, which is not accompanied by chemical changes of

the films, the semiconductor thin films show a pronounced tendency for irreversible agglomeration of the nanocrystals, leading to crystal size increase. The average crystal radii in the case of as-deposited and thermally treated films are given in Table 1, in the next chapter. XRD patterns of the films and bulk precipitates are given in our previous studies [55,58].

3. Electronic transitions in thin films of close-packed ZnSe and CdSe QDs and the SO splitting of the valence band

3.1. Band structure considerations

The band structure of crystals with cubic zinc-blende (sphalerite) lattice is very similar to that of the crystals with diamond structural type [14,16,77]. In the case of zinc-blende semiconductors, the HOMO bands originate primarily from the anionic *p*-orbitals, while LUMO bands originate from the cationic *s*-orbitals. The direct gap is located at $\vec{k} = \{0,0,0\}$ (Γ point of the first Brillouin zone). Neglecting the spin, conduction band is nondegenerate and nearly isotropic, while the valence band has a three-fold degenerate maximum. Inclusion of spin, however, substantially affects the band structure in both qualitative and quantitative sense. In case of compounds including only light elements the electronic spin (S) and angular momentum (L) are both described by good quantum numbers. This is due to the fact that the magnetic field generated by orbiting electron is too weak to induce any coupling with electron spin. When heavier elements are involved in the structure, on the other hand, the nearly relativistic electronic velocities lead to sufficiently large magnetic fields so that L and S are coupled to give a total angular momentum $J = L+S$. The last quantity is now described by good quantum number, in contrast to L and S separately. The general effect of the SO interaction is that it induces a coupling of the electron dynamics in ordinary and spin spaces, which reduces the overall symmetry of the Hamiltonian. In semiconductors of zinc-blende structural type, the SO interaction splits the valence (HOMO) band, which is six-fold degenerate counting the spin, into an upper and lower component (Fig. 1). As can be seen from Fig. 1, the upper (Γ_8) component is four-fold degenerate and it is characterized by the following combinations of quantum numbers characterizing the overall angular momentum and its projection on the *z*-axis: $(J, M_J) = \left(\frac{3}{2}, \pm\frac{3}{2}\right)$ and $\left(\frac{3}{2}, \pm\frac{1}{2}\right)$. The lower ($\Gamma_7$) component is two-fold degenerate and is characterized by $(J, M_J) = \left(\frac{1}{2}, \pm\frac{1}{2}\right)$. In the present study we want to follow the evolution of electronic transitions upon evolution of the average crystal size from strongly quantized to practically non-quantized case of two representatives of the group of zinc-blende structural type

Table 1
The average crystal radii of as-deposited and thermally annealed ZnSe and CdSe quantum dot thin films derived on the basis of XRD data, together with the band-to-band transition energies determined from analyses of the optical absorption spectra

	$\langle R \rangle$, nm	$E_g(\Gamma_8^v \rightarrow \Gamma_6^c)$, eV	$E(\Gamma_7^v \rightarrow \Gamma_6^c)$, eV	$(E-E_g)$, eV
ZnSe				
As-deposited	1.4	3.10	3.50	0.40
Annealed at 150 °C	1.5	2.90	3.30	0.40
Annealed at 200 °C	1.8	2.80	3.20	0.40
Annealed at 250 °C	2.0	2.60	3.00	0.40
CdSe				
As-deposited	2.7	2.08	2.33	0.25
Annealed at 300 °C	12.0	1.77	2.01	0.24

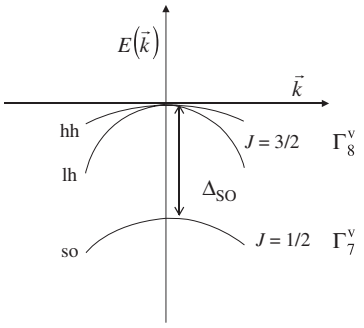

Fig. 1. The valence band in semiconductors of zinc-blende structural type. Δ_{SO}—spin–orbit splitting energy, hh—heavy hole band, lh—light hole band, so—split-off band, $J = L+S$.

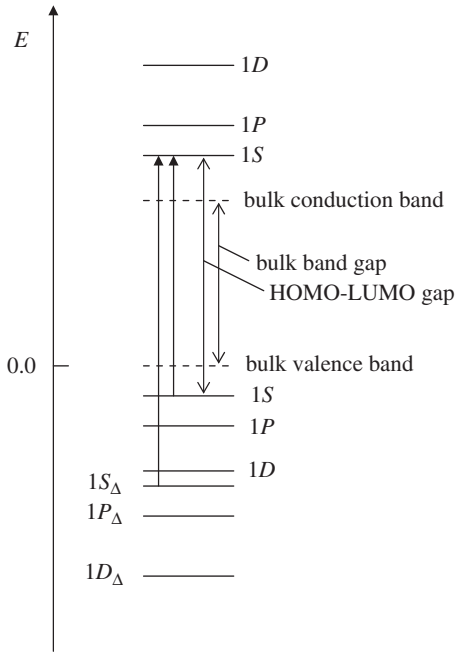

Fig. 2. The discrete hole and electron states arising from valence and conduction bands in the case of semiconductor nanoclusters of zinc-blende structural type according to the simplest model that does not account for the mixing between hole states (according to Ref. [37]).

semiconductors. It is therefore important to have an idea about the influence of size-quantization on the SO split valence band in case of the studied compounds. This problem was actually analyzed some time ago for semiconductor slabs [78,79], as well as more generally [13,38,39,77]. It was concluded that the split-off valence band component Γ_7 is expected to give rise to one series of separate hole states, while the degenerate Γ_8 component is split and quantized due to symmetry lowering. This is schematically presented in Fig. 2. Therefore, two series of quantized hole states are expected to arise upon nanocrystal size decrease, which may be labeled as "heavy holes" and "light holes". The effective masses of the holes are given by

$$m_h = \frac{m_0}{\gamma_1 - 2\gamma_2} \quad (1)$$

$$m_l = \frac{m_0}{\gamma_1 + 2\gamma_2} \quad (2)$$

In the previous equations, m_0 is the free electron mass while γ_1 and γ_2 are the Luttinger parameters characterizing the band shape

[14–16]. In fact, the outlined results are in line with those obtained by Luttinger and Kohn [80] for bulk specimen. These authors have originally introduced three parameters γ_1, γ_2 and γ_3 besides the SO splitting energy to describe the corresponding bulk band structure. Rigorously speaking, the description of the valence band in the manner of Luttinger and Kohn leads to a small warping of this band which is proportional to $(\gamma_2-\gamma_3)$. Usually this small anisotropy is neglected and setting $\gamma_1=\gamma_2=\gamma_3$ one obtains the usual description of the heavy-hole and light-hole band (four-fold degenerate at Γ point, including spin—with the effective masses given by (1) and (2)) and a split-off band with an (isotropic) effective mass given by

$$m_s = m_i = \frac{m_0}{\gamma_1} \tag{3}$$

3.2. Experimentally detected optical transitions

In order to characterize the band-to-band electronic transitions (in the case of films constituted of practically non-quantized QDs) and the transitions between the discrete hole and electron states arising from the valence and conduction bands (in case of quantized QD films), we have recorded the optical absorption spectra of the films with glass substrate taken as a reference sample. On the basis of experimentally measured spectral dependence of the transmission coefficient ($T=f(h\nu)$), we have constructed the spectral dependence of absorption coefficient (i.e. the function $\alpha=f(h\nu)$) using the following formula:

$$\alpha(h\nu) = d^{-1}\ \ln(T(h\nu))^{-1} \tag{4}$$

In the last equation, d is the thickness of the thin film determined gravimetrically or interferometrically. The spectra processing was performed using the MS EXCEL software package [81]. Since the size-quantization is not expected to affect the *type* of band-to-band transitions, the optical absorption data were converted to the semiconductor absorption function for direct dipole-allowed band-to-band electronic transitions of the type [16,81–86]:

$$(\alpha h\nu)^2 = A(h\nu - E_g) \tag{5}$$

In Eq. (5), A is a constant which arises from Fermi's golden rule for fundamental band-to-band electronic transitions within the framework of parabolic approximation for the dispersion relation [16,81–86]. Further, linear least-squares interpolations of the $(\alpha h\nu)^2$ vs. $h\nu$ dependencies were carried out in the relevant energy ranges. Linear interpolations were carefully performed, with successive inclusion or elimination of a number of neighboring points in the correlation ranges and parallelly monitoring the R^2 value. After determination of the sets of relevant points which belong to the linear $(\alpha h\nu)^2$ vs. $h\nu$ dependence, we have extrapolated $(\alpha h\nu)^2$ vs. $h\nu$ dependences to $\alpha h\nu=0$ and calculated the corresponding transition energies on the basis of previously derived correlation equations. The semiconductor absorption functions of the type $(\alpha h\nu)^2=f(h\nu)$ in the case of as-deposited and thermally treated ZnSe and CdSe QD thin films are presented in Figs. 3 and 4. Besides the standard semiconductor absorption function for dipole-allowed direct band-to-band transitions of the mentioned form, we have also constructed the functions of the form $\alpha h\nu=f(h\nu)$. Some authors have reported that the functions of the last type are more suitable for description of transitions between extended states in amorphous semiconductors [87]. Although such statement has also been supported by some theoretical analyses, it has not been confirmed as a general rule. In the case of the presently studied systems, actually worse fit was obtained when $\alpha h\nu$ vs. $h\nu$ dependencies were used instead of the $(\alpha h\nu)^2=f(h\nu)$ ones. Therefore, all of the results, which will be further presented, are based on analyses of the "standard" semiconductor absorption functions. In this context, it is worth mentioning that we have also constructed other dependencies of the type

$$(\alpha h\nu)^n = \text{const.}(h\nu - E_g) \tag{6}$$

for all physically possible values of n (besides 2, also $\frac{1}{2},\frac{2}{3},\frac{1}{3}$), corresponding to direct and indirect dipole-allowed and forbidden transitions respectively. However, linear dependence in appreciable energy range was obtained only in the case of $n=2$. The experimental results are summarized in Table 1.

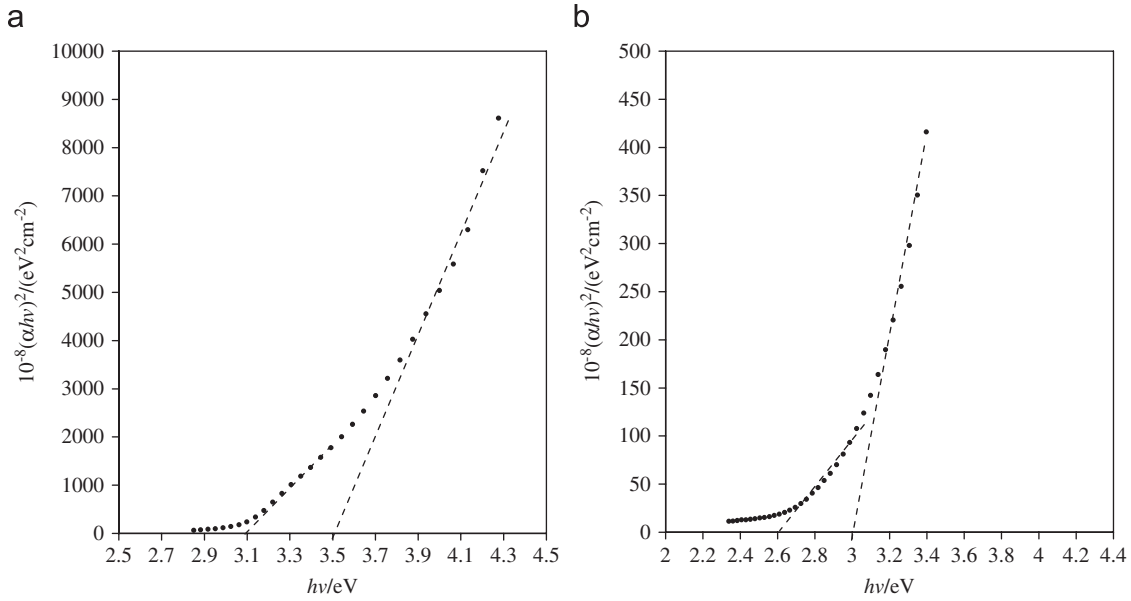

Fig. 3. The plots of $(\alpha h\nu)^2$ vs. $h\nu$ for as-deposited (a) and thermally treated ZnSe quantum dot thin films at 250 °C (b), together with the corresponding extrapolations to $\alpha h\nu=0$.

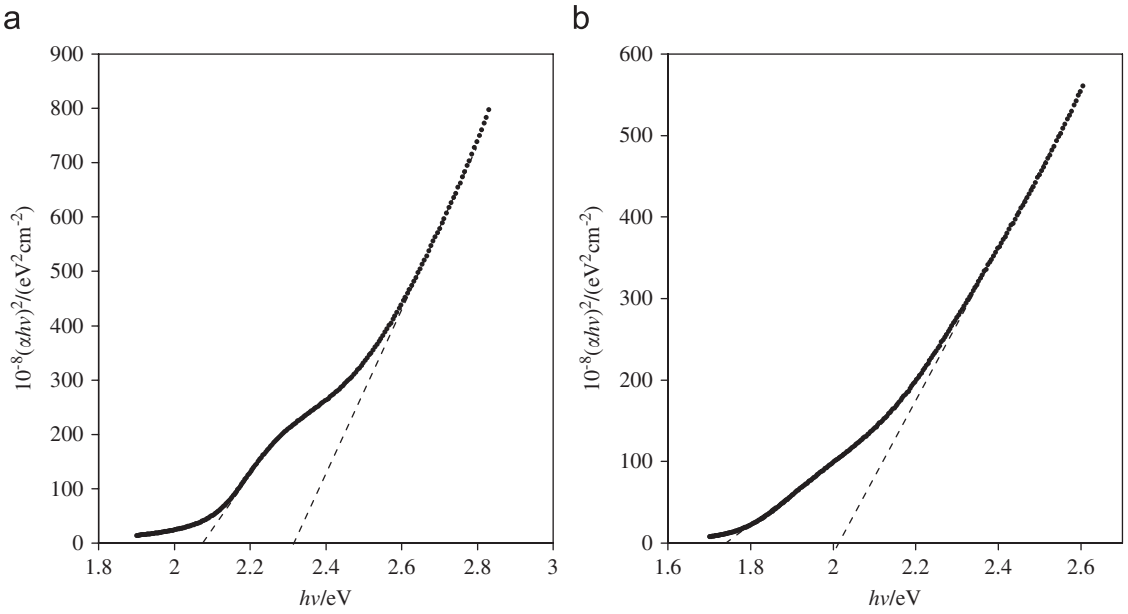

Fig. 4. The plots of $(\alpha h\nu)^2$ vs. $h\nu$ for as-deposited (a) and thermally treated CdSe quantum dot thin films at 300 °C (b), together with the corresponding extrapolations to $\alpha h\nu = 0$.

3.3. *A simple explanation of electronic transitions accounting for the SO splitting of the valence band*

In order to make a proper assignment of the experimentally detected electronic transitions, we firstly consider the simplest model of semiconductor cluster electronic structure, following the results of Brus et al. [13,30,37]. Within this model, the quantum-confined states for electron–hole pair can be calculated employing the effective mass approximation. Simply speaking, the bulk solid energy bands are transformed into discrete sets of cluster molecular orbitals, which are well separated. These energy levels, corresponding to the resulting particle-in-a-sphere wavefunctions (assuming spherical cluster shapes), are labeled according to their symmetry. Since the conduction band is nondegenerate (ignoring spin) and almost isotropic near its absolute minimum at $\vec{k} = \{0,0,0\}$ (i.e. the corresponding effective mass is a scalar), the lowest few discrete particle-in-a-sphere levels are characterized by radial (N) and angular (L) quantum numbers. It should be emphasized that there is no apparent analogy with the hydrogen atom situation since the potential in this case is not Coulombic. Considering the energy levels near the absolute maximum of the valence band, similarly as in the case of the bulk semiconductor, the situation gets much more complicated. Basically, the SO split valence band gives rise to two sets of occupied states (Fig. 2). Except at $\vec{k} = \{0,0,0\}$, these bands can be described by a 6×6 tensor Hamiltonian, which, as shown by Brus et al. following the approach by Baldereshi and Lipari [15,30], in a spherical harmonic basis may be written in the form

$$\hat{H}_{\mathrm{h}} = \hat{H}_S + \hat{H}_D \tag{7}$$

$\hat{H}_S$ is a diagonal matrix containing S-type hole momentum operators and the SO splitting energy Δ [15,30]. In this operator, only the isotropic hole mass defined before by (3) is actually included. $\hat{H}_D$, on the other hand, contains the d-like operators and it is nondiagonal. If this term in (7) is ignored, two series of discrete hole states arise which are offset by a SO splitting energy Δ (Fig. 2). The spin, N, L, and the total angular momentum J ($J = L+S$) are individually all good quantum numbers. In such case, it is the single isotropic hole mass that governs the dependence of the positions of these levels upon particle size change. The lowest-lying occupied hole states, according to this discussion, are the $1S$ and $1S_\Delta$ (i.e. the Γ_8 $1S$ and the Γ_7 $1S$ level). In absence of any mixing, both of these levels would be expected to remain relatively pure, regardless on the semiconductor nanocrystal size. Upon particle size decrease, both of these states are expected to shift together (simultaneously) to higher energy via the isotropic hole mass. The lowest "band to band" transitions in the very small nanoclusters, as well as in the bulk-like clusters are thus $1S \rightarrow 1S$ and $1S_\Delta \rightarrow 1S$. The two transitions should be split by a value Δ, which is expected to be similar to the value of the SO splitting energy characteristic for bulk material.

By analysis of the UV–VIS spectra for the films constituted by three-dimensional arrays of ZnSe QDs characterized with the smallest average nanocrystal size, we have indeed observed two lowest-lying electronic transitions (at 3.10 and 3.50 eV—Fig. 3a) split by Δ. According to the previous discussion, they may be attributed to the $1S \rightarrow 1S$ and $1S_\Delta \rightarrow 1S$ transitions denoted by arrows in Fig. 2. The "next" allowed $1P \rightarrow 1P$ transitions are expected to be considerably further blue-shifted. As can be seen from Table 1, although there is an overall red-shift of both transition energies upon average crystal size increase (not accompanied by any changes in the chemical composition of the films), the energy difference between them remains unchanged. Thus, both of the energetically lowest-lying electronic transitions in the case of ZnSe QDs in thin film form are blue-shifted with respect to the expected transitions in the case of bulk material, but the splitting between them (which is according to this simple model essentially solely due to the SO interaction) remains practically unchanged.

Essentially the same situation is observed in the case of thin films constituted of close-packed CdSe QDs. In this case, the energy difference between the first two electronic transitions is almost twice smaller than in ZnSe (Table 1). If the assignment outlined before was correct, this energy would correspond to the SO splitting energy of the valence band in CdSe. The bulk (macrocrystalline) value for this quantity, on the other hand, is expected to be similar to that in the case of ZnSe (about 0.40 eV [30]). The SO splitting of the valence band is a phenomenon governed solely by the selenide anion, i.e. it is in a sense of an

"atomic" and not crystalline nature. However, our experimental data for the energy splitting between the first two "band-to-band" transitions in the case of CdSe QD thin films seem to be in good agreement with other recently published data in the literature [23–26,28,29,31–33,35,43,44]. Thus, although the outlined simple reasoning explains quite nicely the independence of the Δ value on the average nanocrystal size, the previous seeming inconsistency of Δ for the two studied semiconductors clearly shows that it is impossible to rely solely on such simple theory if one wants to make a more profound analysis of the optical spectroscopic data for QD thin films.

The finding that the apparent SO splitting energy Δ in semiconductor QDs does not depend on the nanocrystal (QD) size has actually been mentioned in some theoretical papers (see, e.g., Ref. [88]), in the context of development or implementation of numerical quantum theoretical methods for computation of the QD energy level structure and its evolution with the QD size. However, all of these analyses were implemented for isolated QDs (to compare with experimental data obtained for colloidal QDs). In this respect, thus, our experimental data allow such conclusion to be extended to the case of thin solid films composed by close-packed QDs. As we will discuss later, however, one should cautiously assign the electronic transitions in cases of semiconductor QDs for which energy level mixing may occur. In such systems, the parameter Δ may not be straightforwardly derivable from the energy level differences detected by spectroscopic techniques.

Up to now we have not discussed one extremely important issue concerning the overall appearance of the optical absorption spectra of the studied QD thin films. If we consider electronic transitions between molecular-like energy levels in QDs, then the absorption spectra should contain absorption bands. Instead, as can be seen from Figs. 5 and 6, the spectral appearances closely resemble the case of bulk-like materials (except for the blue-shifts of optical absorption onsets), i.e. they are essentially structureless. This observation will be explained in the following chapter.

3.4. The more profound physical picture, accounting for the hole energy levels mixing

When the QD sizes are such that one enters the strong confinement regime of electrons and holes, the charge carriers may be treated quite independently. Physically, this means that the confinement energy is much larger than the energy of

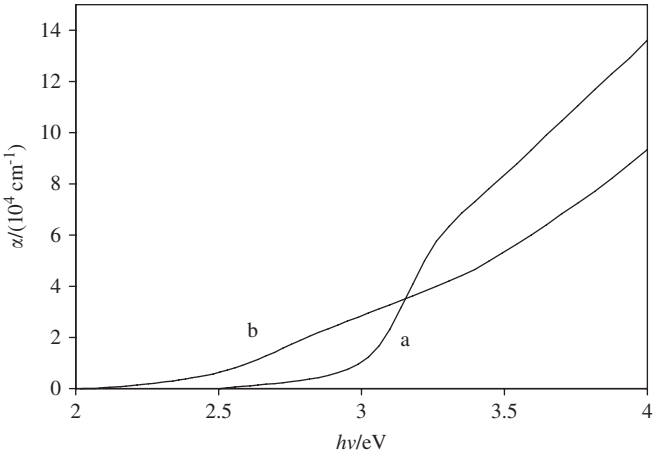

Fig. 5. The spectral dependence of the absorption coefficient for as-deposited (a) and thermally treated ZnSe quantum dot thin films at 250 °C (b).

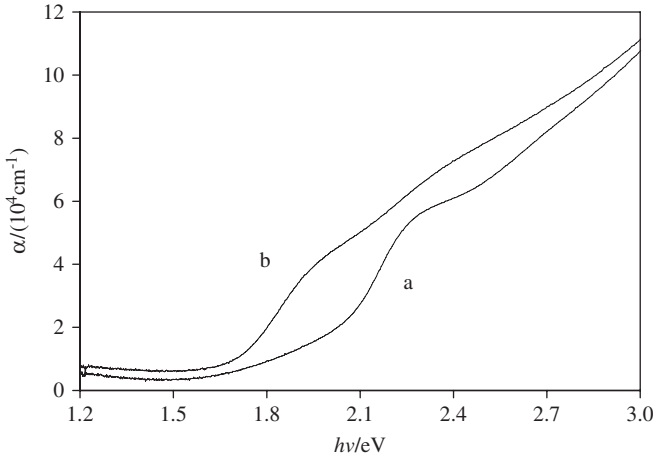

Fig. 6. The spectral dependence of the absorption coefficient for as-deposited (a) and thermally treated CdSe quantum dot thin films at 300 °C (b).

Coulomb interaction between these particles. In this regime, the electron and hole wavefunctions are represented as a product of unit-cell basis function and an envelope function. The envelope function satisfies the spherical boundary conditions. It is intuitively clear that it could be assumed that the unit-cell component is identical to the case of a bulk material. The actual effort in explanation of the QD energy level structure is therefore focused on determination of the envelope function [38,39]. Let us, for the beginning, consider a simple two-band isotropic effective mass model as an approximation to the bulk valence and conduction bands. If we assume that the charge carrier motions are confined by an infinitely high potential barrier at QD boundaries, both electrons and holes may be described by "particle in a sphere" envelope functions [38,39]. These envelope functions are labeled by the radial quantum numbers (N_h i.e. N_e) and the angular momenta (L_h i.e. L_e). The total QD wavefunction, within this approach, is a simple product between the individual electron and hole components. For example, the first excited state may be denoted as ($1S_h$, $1S_e$). In this state, the hole and the electron are in their *S*-like envelope functions and both radial quantum numbers are equal to 1. However, accounting for the complexities in the band structures of the studied zinc-blende semiconductors, as described by the Luttinger–Kohn approach, the following additional important conclusions could be derived. When the Luttinger–Kohn Hamiltonian is combined with a spherical potential in the spherical band approximation, certain mixing between bulk valence bands occurs. This mixing of states becomes particularly important upon particle size decrease (i.e. going from bulk materials to QDs). Accounting explicitly for this energy level mixing phenomena, one arrives at the following main results. In this case, the only good quantum numbers for the envelope wavefunction are the parity and total hole angular momentum $F = L_h + J$. J is the Bloch band-edge angular momentum ($\frac{3}{2}$ for the light and heavy hole bands and $\frac{1}{2}$ for the split-off band), while L is the envelope angular momentum. The hole states within a QD have contributions from spherical harmonics described by L_h and $L_h + 2$. This observation is commonly referred to as the "*S*–*D* mixing". Also, there are certain contributions from the heavy-hole, light-hole and split-off valence subbands to a given hole QD energy level. Within this advanced treatment, the QD hole states are labeled as N_hL_F, where L_F denotes the combination of L and $L + 2$ spherical harmonics having a total angular momentum *F*. The electronic envelope functions, on the other hand, are not affected by the valence band complexities. They are still labeled as N_eL_e. Within this approach, the first excited state in a QD

nanocrystal is denoted as $(1S_{3/2}, 1S_e)$. Due to the previously mentioned mixing between hole states, this level contains contributions from the following three hole components: $(F=\frac{3}{2}, J=\frac{3}{2}, L_h=0)$, $(F=\frac{3}{2}, J=\frac{3}{2}, L_h=2)$ and $(F=\frac{3}{2}, J=\frac{1}{2}, L_h=2)$. Advanced quantitative theoretical treatments of the mentioned aspects have been published in the series of works of Bawendi et al. [28,29,33–36]. In their papers, even the nonparabolicity of the bands as well as the finiteness of the barrier height at QD edge were taken into account. These treatments are in fact analogous to the early works of Brus et al. [30] concerning ZnSe QDs in which the $\hat{H}_D$ term in (7), causing certain mixing of the QD energy levels, has been taken explicitly into account.

According to the previous discussion concerning the actual existence of a series of states split from the first excited state $(1S_{3/2}, 1S_e)$ by the influence of SO coupling and size-quantization effects on the band structure of zinc-blende type ZnSe and CdSe semiconductors, on the basis of quantitative results outlined in Refs. [33–46], we make the following assignments of the observed electronic transitions in our two cases. Without any doubt, we attribute the lowest-energy electronic transition in quantized films to the ground state—$(1S_{3/2}, 1S_e)$ transition in the nanocrystals. As can be inferred from Table 1, this transition is strongly blue-shifted with respect to the bulk value in the case of both of the studied systems—ZnSe and CdSe. The blue-shift is due to three-dimensional quantum confinement effects in ZnSe and CdSe QD thin films. A further confirmation of the last statement is the fact that upon particle size increase due to high-temperature annealing (which is not accompanied by changes in chemical composition of the QD films) the ground state—$(1S_{3/2}, 1S_e)$ transition energy exhibits a continual red-shift. It eventually converges to the bulk band gap energy corresponding to the $\Gamma_8^v \rightarrow \Gamma_6^c$ interband electronic transition in essentially non-quantized samples. As can be inferred from Table 1, the confinement energies ($\Delta E = E(1S_{3/2}, 1S_e) - E_{g,bulk}$) in the presently studied QD film samples are large, i.e. the films are strongly quantized. As mentioned before, it would be therefore expected that the optical absorption spectra should exhibit pattern characteristic of discretized energy levels in individual QDs (i.e. the excitonic peaks should be clearly visible in the absorption spectra). Such patterns are, however, not present in the optical absorption spectra of CdSe and ZnSe QD thin films (Figs. 5 and 6). We attribute the observance of a structureless absorption spectrum in the studied two cases to the formation of collective electronic states in an ensemble of QDs, which are delocalized within a finite number of nanocrystals. Such states are formed as a result of the interdot electronic coupling—a phenomenon that seems to determine the complete optical properties of close-packed nanocrystallites (e.g. in thin films form). More detailed and seriously founded studies of interdot couplings occurring in the case of close-packed QD solids have been carried out only recently [23–26]. According to these recently accumulated data, the interdot electronic coupling occurs when very small QDs are close-packed. The basic mechanism of the coupling is the tunneling one, i.e. due the charge carrier leakage outside each nanoparticle constituting the QD ensemble. From the viewpoint of the optical properties of QD thin films, this interdot coupling is manifested through broadening of the exciton peak in comparison to the case of diluted ensembles of QDs. We have analyzed in detail the evolution of the confinement energy upon particle size increase in the case of ZnSe and CdSe QD thin films [53–58]. In this context, we have demonstrated that it is of crucial importance to account for the charge carrier leakage outside the nanoparticles (by tunneling mechanism) to get a sufficiently good agreement of theoretical predictions with the experimentally measured values of ΔE [54], which seems to be in line with the previously outlined argument concerning interdot electronic couplings.

The correct assignment of higher-energy electronic transitions in quantized ZnSe and CdSe films appears to be a much more complex task. According to Refs. [33–46], the second excited state in zinc-blende semiconducting QDs is the $(2S_{3/2}, 1S_e)$ one. However, the expected energy differences between the ground state—$(1S_{3/2}, 1S_e)$ and ground state—$(2S_{3/2}, 1S_e)$ electronic transitions are less than 0.1 eV (for ground state—$(1S_{3/2}, 1S_e)$ transition energies of about 2.08 eV). Also, the ground state—$(2S_{3/2}, 1S_e)$ transition energy is expected to depend linearly on the ΔE(ground state—$(1S_{3/2}, 1S_e)$). We thus rule out the possibility that the second clearly differentiated feature of the absorption spectra of CdSe and ZnSe QD thin films could correspond to the ground state—$(2S_{3/2}, 1S_e)$ electronic transition. It is, however, possible that this transition feature is masked by the much stronger ground state—$(1S_{3/2}, 1S_e)$ one. By carefully reanalyzing the $(\alpha h\nu)^2$ vs. $h\nu$ dependence in the energy region just above the absorption onset in the case of CdSe thin films of closely packed QDs, we have indeed observed an additional inflection point (although much less clearly differentiated; Fig. 7). According to the energy difference between this and the fundamental ground state—$(1S_{3/2}, 1S_e)$ transition, it is likely that it corresponds to the ground state—$(2S_{3/2}, 1S_e)$ electronic transition. We were unfortunately unable to detect this transition in the case of ZnSe films. The third excited state, according to energy ordering [33–46], should be $(1S_{1/2}, 1S_e)$. For thin films of close-packed CdSe QDs, the ground state—$(1S_{1/2}, 1S_e)$ transition energy should be much less size-dependent than the ground state—$(2S_{3/2}, 1S_e)$ one. The agreement of our optical spectroscopy data with the predictions given in Refs. [33–46] is excellent, and we could thus assign the second feature in the absorption spectra of our CdSe thin films exactly to the ground state—$(1S_{1/2}, 1S_e)$ electronic transition. However, Woggon and collaborators have given a rather important note in Ref. [44], on the basis of their investigations of optical transitions in CdSe QDs which employed photoluminescence, pump-probe and photoluminescence excitation spectroscopies. According to these authors, in the case of QDs with average sizes smaller than Bohr's excitonic radius, the $(2P_{3/2}, 1P_e)$ state could possibly appear much closer in energy to $(2S_{3/2}, 1S_e)$ than $(1S_{1/2}, 1S_e)$. Such reasoning is supported by the fact that the previously mentioned energy ordering of the electron–hole excited states in CdSe QDs are based on theoretical approaches which are of questionable validity for P states. Therefore, in the case of very small nanocrystals the situation concerning the correct assignments of electronic transitions may be further complicated. Unfortunately, such an in-depth analysis

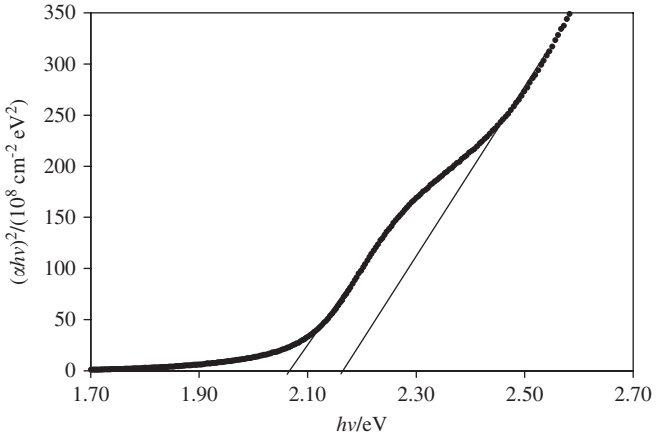

Fig. 7. The $(\alpha h\nu)^2$ vs. $h\nu$ dependence in the energy region just above the absorption onset in the case of CdSe thin films of closely packed QDs. The additional, much less clearly differentiated inflection point corresponds to the ground state—$(2S_{3/2}, 1S_e)$ electronic transition.

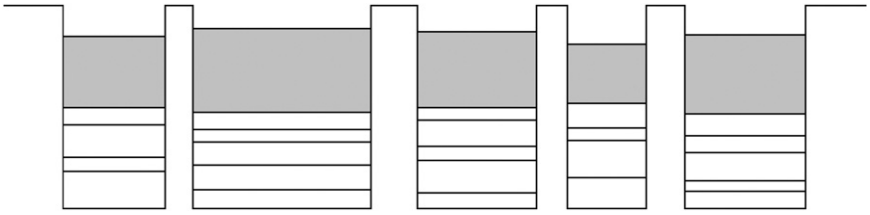

Fig. 8. Schematic depiction of one-dimensional multiple quantum well structure consisting of a random arrangement of different wells.

for QD hole energy levels as provided in Refs. [33–46] for CdSe has not been carried out for ZnSe. However, according to the existing literature data the assignment of the second observable transition in this system should be performed analogously as in CdSe. Now, we go back to the apparent "problem" of the different splittings between the first two observed transition energies in ZnSe and CdSe QDs, which could not be explained within the simple approach given in Chapter 3.3. At first sight, it seems that the detected "energy splittings" should correspond to the SO splitting energy of the zinc-blende valence bands. As mentioned before, as the SO splitting is an atomic phenomenon, no differences between the measured values are expected between CdSe and ZnSe films. However, if one accounts for the apparent mixing of hole energy levels within QDs, it is clear that the observed "splittings" do not correspond exactly to SO splitting energies in both semiconductors, but are rather complex functions of the last quantity. The exact position of each hole energy level depends, besides on the "SO splitting energy", also on other material-characteristic parameters. The seeming discrepancy between expectations and experimental data is thus eliminated in the light of more profound analyses of the QD hole energy spectra.

The ground state—$(1S_{1/2}, 1S_e)$ transition energy also exhibits a red-shift upon high temperature annealing treatment of the films. It would be expected that this particular transition should converge to the $\Gamma_7^v \rightarrow \Gamma_6^c$ interband electronic transition in bulk zinc-blende semiconductors, which should occur at $E_g+\Delta_0$ (where Δ_0 is the SO splitting energy of the valence band in the case of bulk semiconductor specimen). In the case of ZnSe QD thin films, the energy difference between the ground state—$(1S_{1/2}, 1S_e)$ and the ground state—$(1S_{3/2}, 1S_e)$ transitions is 0.40 eV. This value remains practically unchanged upon variations in QD size and is in very good agreement with the literature value for the SO splitting energy of a bulk specimen of zinc-blende polymorph modification of this semiconductor [64]. One is thus lead to a conclusion that the hole energy level mixing in the case of ZnSe QDs is not as significant as in CdSe, i.e. the states are purer in the former case.

The energy difference between the ground state—$(1S_{1/2}, 1S_e)$ and the ground state—$(1S_{3/2}, 1S_e)$ transitions in the case of essentially non-quantized CdSe films found in the present study, on the other hand, is somewhat smaller than the literature value for the SO splitting for the hexagonal (wurtzite) polymorph of this semiconductor. Since the SO coupling is essentially an intraatomic phenomenon, it is expected that the magnitude of the SO splitting of the valence band in this case should not depend drastically on the crystal structure of the compound in question. Janowitz et al. [89] have estimated the SO splitting energy of the valence band in the case of cubic modification of CdSe, on the basis of their analysis of the pseudodielectric function of this material. They obtained a value of 0.41 eV, which is quite close to the Δ for wurtzite sample, in line with the previous discussion. Their analysis was, however, based on the second derivative spectra calculated for MBE-grown CdSe films on GaAs substrates. The presence of interference fringes due to the finite thickness and low absorption coefficient of CdSe films in the energy range below 2.5 eV has complicated the analysis of the pseudodielectric function, which also included contributions from GaAs substrate. Other authors, such as Velumani et al. [31] have reported much smaller, thickness-dependent values for the SO splitting energy in the case of CdSe films deposited on ITO substrates at various temperatures, ranging from 0.03 to 0.13 eV. Even such a brief retrospective of literature data certainly indicates that the question on the exact magnitude of the valence band SO splitting energy in this semiconductor has not been unequivocally solved yet, or that this quantity depends on the exact route employed to synthesize this semiconducting compound. In our study, we deal with thin films of close-packed CdSe QDs. In the weak confinement regime, characteristic for films with average crystal radii of more than 15 nm, although the quantum confinement effects on the absorption onset are absent, the hole energy level mixing may still be very significant. Therefore, the observed difference between the ground state—$(1S_{1/2}, 1S_e)$ and the ground state—$(1S_{3/2}, 1S_e)$ transition energies may still not correspond to the exact SO splitting energy characteristic for this semiconductor.

It is not clear, at least not in a quantitative manner, how should the close packing of the QDs affect the exact positions of the hole and electron energy levels in three-dimensional assemblies of QDs deposited as thin films. Generally speaking, when nanocrystals are assembled and form a macroscopic colloidal crystal (a QD solid) one deals with a kind of condensed matter with spatial organization on a length scale comparable to the electron de Broglie wavelength. Considering the dense QD ensembles as analogous structures to multiple QWs, actually the QD solid may be viewed as a three-dimensional superlattice formed by QDs as basic building blocks. Ensembles of densely packed QDs deposited as thin films are expected to resemble the energy band structures of "conventional" solids. This implies an existence of energy bands in a perfect three-dimensional superlattice and coexistence of both localized and delocalized states in a lattice with some degree of disorder. These concepts are illustrated in Fig. 8, in which one-dimensional multiple QW structure is depicted, consisting of a random arrangement of different wells. The real nanocrystal assembly that we deal with is a three-dimensional analogue of Fig. 8. In comparison to an assembly of isolated QDs, it is expected that such a structure should exhibit a slight red-shift of optical absorption onset and a structureless appearance of the optical spectra. Even if the distribution function characterizing the random arrangement of different wells was known, it would be a very difficult task to predict quantitatively the influence of such ordering on the issues related to SO splitting discussed before. Much more involved theoretical insights are required for such a purpose.

4. Conclusions

Optical properties of three-dimensional arrays consisting of ZnSe and CdSe QDs close-packed in thin film form were studied. To make precise assignments of the detected optical transitions and to explain the overall appearances of optical absorption spectra of the films, the size-quantization effects on electron and

hole energy levels were taken into account, along with the collective effects in the colloidal crystals (QD solids). Simple models of three-dimensional confinement effects (which neglect the *S–D* mixing of the hole energy states) lead to conclusion that the two lowest-energy "band-to-band" electronic transitions occur between the 1*S* discrete hole and electronic states, the former arising from bulk valence band Γ_8 and Γ_7 components which are split due to SO interaction ($1S \rightarrow 1S$ and $1S_{\Delta} \rightarrow 1S$). The observed splitting between these two electronic transitions remains unaffected by variations of QDs average size. Such simple model was, however, found to be incapable of explaining the substantial differences in the measured splitting energy between ZnSe and CdSe. Accounting for the *S–D* mixing of the hole energy states, on the other hand, allows a more consistent explanation of the experimental observations. The most prominent absorption onsets, according to the latest approach, correspond to the ground state—($1S_{3/2}$, $1S_e$) and ground state—($1S_{1/2}$, $1S_e$) electronic transitions. The transition involving the second higher excited ($2S_{3/2}$, $1S_e$) state appears to be masked by the ground state—($1S_{3/2}$, $1S_e$) transition. Due to the mixing between hole states, each hole level within the nanocrystals contains contributions from various other hole levels, and therefore the observed energy differences between two subsequent electronic transitions are not equal to the SO splitting energy of the valence bands.

References

[1] L.E. Brus, J. Phys. Chem. 90 (1986) 2555.
[2] A.D. Yoffe, Adv. Phys. 50 (2001) 1.
[3] A.D. Yoffe, Adv. Phys. 51 (2002) 799.
[4] R. Memming, Semiconductor Electrochemistry, Wiley-VCH, Weinheim, 2001.
[5] L.E. Brus, J. Chem. Phys. 79 (1983) 5566.
[6] L.E. Brus, J. Chem. Phys. 80 (1984) 4403.
[7] A.L. Efros, A.L. Efros, Fiz. Tekh. Poluprovodn. 16 (1982) 1209.
[8] Y. Wang, N. Herron, J. Phys. Chem. 95 (1991) 525.
[9] P.E. Lippens, M. Lanoo, Phys. Rev. B 39 (1989) 10935.
[10] Y. Kayanuma, Phys. Rev. B 38 (1988) 9797.
[11] Y. Wang, A. Suna, W. Mahler, R. Kasowski, J. Chem. Phys. 87 (1987) 7315.
[12] Y. Nosaka, J. Phys. Chem. 95 (1991) 5054.
[13] M.G. Bawendi, M.L. Steigerwald, L.E. Brus, Ann. Rev. Phys. Chem. 41 (1990) 477.
[14] M. Cardona, J. Phys. Chem. Solids 24 (1963) 1543.
[15] A. Baldereshi, N.G. Lipari, Phys. Rev. B 3 (1971) 439.
[16] P.Y. Yu, M. Cardona, Fundamentals of Semiconductors, Springer, Berlin, 1999.
[17] E. Tsitsishvilli, G.S. Lozano, A.O. Gogolin, Phys. Rev. B 70 (2004) 115316.
[18] J.P. Heida, B.J. van Wees, J.J. Kuipers, T.M. Klapwijk, G. Borghs, Phys. Rev. B 57 (1998) 11911.
[19] T. Dietl, H. Ohno, F. Matsakura, J. Cibert, D. Ferrand, Science 287 (2000) 1019.
[20] S.A. Wolf, D.D. Awschalom, R.A. Buhrman, J.M. Daughton, S. von Molnar, M.L. Roukes, A.Y. Chtchelkanova, D.M. Treger, Science 294 (2001) 1488.
[21] S. Datta, B. Das, Appl. Phys. Lett. 56 (1990) 665.
[22] N. Zaitseva, Z.R. Dai, F.R. Leon, D. Krol, J. Am. Chem. Soc. 127 (2005) 10221.
[23] D.I. Kim, M.A. Islam, L. Avila, I.P. Herman, J. Phys. Chem. B 107 (2003) 6318.
[24] M.V. Artemyev, A.I. Bibik, L.I. Gurinovich, S.V. Gaponenko, H. Jaschinski, U. Woggon, Phys. Stat. Sol. (B) 224 (2001) 393.
[25] M.V. Artemyev, U. Woggon, H. Jaschinski, L.I. Gurinovich, S.V. Gaponenko, J. Phys. Chem. B 104 (2000) 11617.
[26] M.V. Artemyev, A.I. Bibik, L.I. Gurinovich, S.V. Gaponenko, U. Woggon, Phys. Rev. B 60 (1999) 1504.
[27] M.V. Artemyev, V. Sperling, U. Woggon, J. Appl. Phys. 81 (1997) 6975.
[28] C.R. Kagan, C.B. Murray, M. Nirmal, M.G. Bawendi, Phys. Rev. Lett. 76 (1996) 1517.
[29] C.R. Kagan, C.B. Murray, M.G. Bawendi, Phys. Rev. B 54 (1996) 8633.
[30] N. Chestnoy, R. Hull, L.E. Brus, J. Chem. Phys. 85 (1986) 2237.
[31] S. Velumani, X. Mathew, P.J. Sebastian, Sa.K. Narayandass, D. Mangalaraj, Solar Energy Mater. Solar Cells 76 (2003) 347.
[32] P. Němec, D. Mikeš, J. Rohovec, E. Uhlířová, F. Trojánek, P. Malý, Mater. Sci. Eng. B 69–70 (2000) 500.
[33] D.J. Norris, A. Sacra, C.B. Murray, M.G. Bawendi, Phys. Rev. Lett. 72 (1994) 2612.
[34] D.J. Norris, Al.L. Efros, M. Rosen, M.G. Bawendi, Phys. Rev. B 53 (1996) 16347.
[35] D.J. Norris, M.G. Bawendi, Phys. Rev. B 53 (1996) 16338.
[36] M.G. Bawendi, W.L. Wilson, L. Rothberg, P.J. Carroll, T.M. Jedju, M.L. Steigerwald, L.E. Brus, Phys. Rev. Lett. 65 (1990) 1623.
[37] A.P. Alivisatos, A.L. Harris, N.J. Levinos, M.L. Steigerwald, L.E. Brus, J. Chem. Phys. 89 (1988) 4001.
[38] A.I. Ekimov, F. Hache, M.C. Schanne-Klein, D. Ricard, C. Flytzanis, I.A. Kudryavtsev, T.V. Yazeva, A.V. Rodina, Al.L. Efros, J. Opt. Soc. Am. B 10 (1993) 100.
[39] J. Xia, Phys. Rev. B 40 (1989) 8500.
[40] G. Hodes, A. Albu-Yaron, F. Decker, P. Motisuke, Phys. Rev. B 36 (1987) 4215.
[41] E. Lifshitz, I. Dag, I. Litvin, G. Hodes, S. Gorer, R. Reisfeld, M. Zelner, H. Minti, Chem. Phys. Lett. 288 (1998) 188.
[42] U. Woggon, S. Gaponenko, W. Langbein, A. Uhrig, C. Klingshirn, Phys. Rev. B 47 (1993) 3684.
[43] O. Wind, F. Gindele, U. Woggon, J. Lumin. 72–74 (1997) 300.
[44] U. Woggon, O. Wind, F. Gindele, E. Tsitsishvili, M. Müller, J. Lumin. 70 (1996) 269.
[45] F. Gindele, R. Westphäling, U. Woggon, L. Spahnel, V. Ptatschek, Appl. Phys. Lett. 71 (1997) 2181.
[46] U.E.H. Laheld, G.T. Einevoll, Phys. Rev. B 55 (1997) 5184.
[47] B.S. Kim, M.A. Islam, L.E. Brus, I.P. Herman, J. Appl. Phys. 89 (2001) 8127.
[48] B.S. Kim, L. Avila, L.E. Brus, I.P. Herman, Appl. Phys. Lett. 76 (2000) 3715.
[49] V. Ptatschek, B. Schreder, K. Herz, U. Hilbert, W. Ossau, G. Schottner, O. Rahäuser, T. Bischof, G. Lermann, A. Materny, W. Kiefer, G. Bacher, A. Forchel, D. Su, M. Giersig, G. Müller, L. Spanhel, J. Phys. Chem. B 101 (1997) 8898.
[50] C. Raptis, D. Nesheva, Y.C. Boulmetis, Z. Levi, Z. Aneva, J. Phys.: Condens. Matter 16 (2004) 8221.
[51] B. Pejova, I. Grozdanov, Thin Solid Films 515 (2007) 5203.
[52] B. Pejova, I. Grozdanov, Mater. Chem. Phys. 99 (2006) 39.
[53] B. Pejova, A. Tanuševski, I. Grozdanov, J. Solid State Chem. 178 (2005) 1786.
[54] B. Pejova, I. Grozdanov, Mater. Chem. Phys. 90 (2005) 35.
[55] B. Pejova, A. Tanuševski, I. Grozdanov, J. Solid State Chem. 177 (2004) 4785.
[56] B. Pejova, I. Grozdanov, Mater. Lett. 58 (2004) 666.
[57] B. Pejova, A. Tanuševski, I. Grozdanov, J. Solid State Chem. 174 (2003) 276.
[58] B. Pejova, A. Tanuševski, I. Grozdanov, J. Solid State Chem. 172 (2003) 381.
[59] B. Pejova, I. Grozdanov, Thin Solid Films 408 (2002) 6.
[60] B. Pejova, I. Grozdanov, J. Solid State Chem. 158 (2001) 49.
[61] B. Pejova, I. Grozdanov, Appl. Surf. Sci. 177 (2001) 152.
[62] B. Pejova, M. Najdoski, I. Grozdanov, S.K. Dey, Mater. Lett. 45 (2000) 2694.
[63] B. Pejova, M. Najdoski, I. Grozdanov, S.K. Dey, J. Mater. Chem. 9 (1999) 2889.
[64] A.B. Novoselova (Ed.), Physical and Chemical Properties of Semiconductors, Handbook, 1978.
[65] S.A. Empedocles, D.J. Norris, M.G. Bawendi, Phys. Rev. Lett. 77 (1996) 3873.
[66] C.C. Kim, S. Sivananthan, Phys. Rev. B 53 (1996) 1475.
[67] Y. Ohtake, T. Okamoto, A. Yamada, M. Kongai, K. Saito, Sol. Energy Mater. Sol. Cells 49 (1997) 2699.
[68] A.K. Turner, J.M. Woodcock, M.E. Özsan, Sol. Energy Mater. Sol. Cells 35 (1994) 263.
[69] N.G. Patel, C.J. Panchal, K.K. Makhijia, Cryst. Res. Technol. 29 (1994) 1013.
[70] V.A. Smyntyana, V. Gerasutenko, S. Kashulis, G. Mattogno, S. Reghini, Sensors Actuators 19 (1994) 464.
[71] A. Van Calster, F. Vanfleteren, I. De Rycke, J. De Baets, J. Appl. Phys. 64 (1988) 3282.
[72] B. Bonello, B. Fernandez, J. Phys. Chem. Solids 54 (1993) 209.
[73] J.C. Schottmiller, R.W. Francis, C. Wood, US Patent 3884688, 1975.
[74] B.J. Curtis, H. Kiess, H.R. Brunner, K. Frick, Photogr. Sci. Eng. 24 (1980) 244.
[75] M. Weller, Inorganic Materials Chemistry, Oxford Science Publications, Oxford, UK, 1994.
[76] M.G. Bawendi, A.R. Kortan, M.L. Steigerwald, L.E. Brus, J. Chem. Phys. 91 (1989) 7282.
[77] A. Tomasulo, M.V. Ramakrishna, J. Chem. Phys. 105 (1996) 3612.
[78] J.C. Hensel, G. Feher, Phys. Rev. 129 (1963) 1.
[79] R. Dingle, W. Wiegmann, C.H. Henry, Phys. Rev. Lett. 33 (1974) 827.
[80] J.M. Luttinger, W. Kohn, Phys. Rev. 97 (1955) 869.
[81] N.W. Ashcroft, N.D. Mermin, Solid State Physics, Holt, Rinehart and Winston, New York, 1976.
[82] S.M. Sze, Semiconductor Devices, Physics and Technology, Wiley, New York, 1985.
[83] R. Dalven, Introduction to Applied Solid State Physics, Plenum Press, New York, 1990.
[84] K. Seeger, Semiconductor Physics, Springer, New York, 1997.
[85] M.P. Marder, Condensed Matter Physics, Wiley, New York, 2000.
[86] B. Pejova, in: R.W. Buckley (Ed.), Progress in Solid State Chemistry Research, Nova Science Publishers Inc., New York, 2007.
[87] R.S. Tripathi, L.L. Moseley, T. Lukes, Phys. Stat. Sol. (B) 83 (1977) 197.
[88] H. Fu, A. Zunger, Phys. Rev. B 57 (1998) R15064.
[89] C. Janowitz, O. Günther, G. Jungk, R.L. Johnson, P.V. Santos, M. Cardona, W. Faschinger, H. Sitter, Phys. Rev. B 50 (1994) 2181.